This article has not been copyedited and formatted. The final version may differ from this version.
DMD Fast Forward. Published on December 9, 2010 as doi:10.1124/dmd.110.036178

DMD Manuscript # 36178

Atazanavir metabolism according to CYP3A5 status: An *in vitro – in vivo* assessment

Michael F. Wempe

and

Peter L. Anderson

Department of Pharmaceutical Sciences, University of Colorado Denver, Aurora, CO 80045, USA.

Running Title: Atazanavir metabolites and CYP3A5

Corresponding Author: Peter L. Anderson

Department of Pharmaceutical Sciences

12700 E. 19th Ave

C238 RC2 P15-3001

Aurora, CO 80045

Tel: +1-303-724-6128

Fax: +1-303-724-6135

Email: Peter.Anderson@ucdenver.edu

Number of Text Pages: 14

Number of Tables: 2

Number of Figures: 5

Number of References: 11

Abstract: (241 Words)

Introduction: (224 words)

Discussion (1180 words)

Abbreviations:

Atazanavir (ATV), Human Immunodeficiency Virus (HIV), Acquired Immuno-Deficiency syndrome (AIDS), Pharmacokinetic (PK), High Performance Liquid Chromatography/Ultraviolet spectrometry (HPLC/UV), Liquid Chromatography-Mass Spectrometry/Mass Spectrometry (LC-MS/MS), African-American CYP3A5 Expressors (AA-E), non-African-American CYP3A5 expressors (NAA-E), and non-African-American CYP3A5 non-expressors (NAA-NE), Human Liver Microsome (HLM).

DMD Fast Forward. Published on December 9, 2010 as DOI: 10.1124/dmd.110.036178
This article has not been copyedited and formatted. The final version may differ from this version.

Abstract

The current study was a follow up to an *in vivo* study where atazanavir oral clearance was shown to be dependent on genetically-determined CYP3A5 expression status, but only in non-African Americans (Anderson et al, 2009). This study aimed to identify atazanavir metabolites generated by CYP3A5 and to evaluate this metabolite pattern in the African American versus non-African American CYP3A5 expressors from the previous study. First, the *in vitro* metabolism of atazanavir was evaluated using human liver microsomes (HLM), CYP3A4 and CYP3A5 isoforms. Second, the metabolite pattern generated by CYP3A5 was evaluated in human plasma samples from the previous study. Atazanavir metabolites were analyzed using LC-MS/MS methods. Metabolite AUCs were normalized to atazanavir AUC to generate an AUC ratio. Sixteen metabolites were observed in HLM incubations representing five 'Phase I' biotransformation pathways. Mono-oxidation products (**M1** and **M2**) were formed by CYP3A5 at a faster rate than CYP3A4 by 32- and 2.6-fold, respectively. This finding was replicated in HLMs from a genetically-determined CYP3A5 expressor versus non-expressor. In the *in vivo* samples, the **M1** and **M2** AUC ratios were about 2-fold higher in CYP3A5 expressors versus non-expressors ($P<0.05$) and the difference was similar in African-Americans and non-African Americans. Thus, CYP3A5 produced a unique metabolite 'signature' for atazanavir *in vitro* and *in vivo*, independent of race. Therefore, other pharmacological factors are likely to explain the apparent lack of effect of genetically-determined CYP3A5 expressor status on atazanavir oral clearance in African Americans from the previous study.

Introduction

Atazanavir is a commonly prescribed HIV protease inhibitor that is approved by the FDA for once-daily administration. ATV exhibits significant pharmacokinetic (PK) variability arising from acid-dependent absorption, drug-food/drug-drug interactions, and/or variability in the enzyme systems responsible for its clearance (Croom et al, 2009).

In a previously published study, the influence of genetically-determined CYP3A5 expression on atazanavir PK was assessed in a group of 31 HIV-negative human volunteers (Anderson et al, 2009). Subjects were administered atazanavir 400 mg each morning for 7-days and then a 24 h PK study was conducted following a standardized breakfast. Enrollment was balanced for genetically-determined CYP3A5 expression, race, and gender. The primary finding was that atazanavir oral clearance (CL/F) was 1.39-fold faster in people who expressed CYP3A5 versus those who did not. However, atazanavir CL/F differences were not present in African-American CYP3A5 expressors. This discrepancy raised the question as to whether CYP3A5 expression was exerting a consistent effect in AA and NAA. We hypothesized that an analysis of ATV metabolites could shed light on these *in vivo* findings, and this was the basis for the present study. The aims were to evaluate atazanavir metabolism *in vitro* using human liver microsomes, CYP3A4, and CYP3A5 to define metabolite formation differences for CYP3A5 followed by a comparison of CYP3A5 metabolite profiles in the AA and NAA groups from the previous human PK study.

Materials and Methods

Chemicals and Reagents: Atazanavir sulfate was obtained from the NIH AIDS Research and Reference Reagent Program; Rockville, MD 20850 (Lot # NIH 2 040131). Ritonavir was purchased from Apin Chemicals (Oxon, OX14, 4RU, UK). Human liver microsomes (HLM; 20.0 mg/mL, pool of 50, mixed gender, Lot 0510025; HLM from genetically-determined CYP3A5 non-expressor Lot #0710253; HLM from genetically-determined CYP3A5 expressor Lot #0710272, human CYP3A4 (CYP010; 3A4 low reductase; Batch C3A4LR004; 5.6 nmol CYP/mL; 12.6 mg protein/mL; 444 pmol p450/mg protein), and human CYP3A5 (CYP015; 3A5 low reductase; C3A5LR008; 2.8 nmol CYP/mL; 14.5 mg protein/mL; 193 pmol p450/mg protein) with human CYP-reductase coexpressed in *Escherichia coli* were purchased from Xenotech (Lenexa, Kansas).

***In vitro* experiments:** Incubations consisted of phosphate buffer (100 mM; pH 7.4), $MgCl_2$ (5.0 mM), and EDTA (0.1 mM) and were conducted at 37 ºC. Conditions utilized human microsomes (1.0 mg protein/mL), CYP3A4 (100 pmol p450/mL) or CYP3A5 (100 pmol p450/mL) with atazanavir (10.0 µM) in the presence of NADPH (1.0 mM) for various times (0.5, 5, 10, 15 and 30 min). In the case of human liver microsomes, additional incubations were conducted for 90 min. Other incubations utilized human liver microsomes (0.20 mg protein/mL) in the presence of atazanavir (1.0 µM), ritonavir (0.0, 0.10, 0.25, and 0.50 µM) and NADPH (1.0 mM) for various times (0.5, 5, 10, 20 and 30 min). In all cases, incubate samples (100 µL) were removed and added to quench solution (acetonitrile, 300 µL). The resulting samples were vortexed (5 sec) and centrifuged at 3000 rpm (5.0 min) and subsequently analyzed by LC-MS/MS. The data were expressed as percent disappearance of parent relative to the ~0.5 min time point sample. These results were used to calculate *in vitro* intrinsic clearance values (CL_{int}, reported in units of

DMD Fast Forward. Published on December 9, 2010 as DOI: 10.1124/dmd.110.036178
This article has not been copyedited and formatted. The final version may differ from this version.

µL/min/mg protein), as previously described using the following equation: (0.693/*in vitro* $T_{1/2}$) • (µL incubation/mg microsomal protein) (Obach, 1999).

LC-MS/MS: Atazanavir metabolites were analyzed by LC-MS/MS (Applied Biosystems Sciex 4000 ®, Applied Biosystems; Foster City, CA; Shimadzu HPLC, Shimadzu Scientific Instruments, Inc.; Columbia, MD; Leap auto-sampler, LEAP Technologies; Carrboro, NC). Liquid chromatography employed an Agilent Technologies, Zorbax extended-C18 250 x 4.6 mm, 5 micron column at 40.0 ± 0.1 ^{o}C with a flow-rate of 0.4 mL/min. The mobile phase consisted of A: 10 mM ammonium acetate, 0.1% formic acid in water, and B: 50:50 acetonitrile:methanol. Chromatography consisted of 95% A for 0.10 min; brought to 50% B at 1.50 min and held for 2.50 min; ramped to 80% B at 11.50 min, and then to 95% B at 12.00 min and held for 7.50 min, and finally brought back to 95% A at 22.50 min and held for 3.5 min (26.0 min total run time). An atazanavir sulphate stock DMSO solution (20 mM) was freshly prepared and used to generate the atazanavir standard curve (linear range; 0.05 to 950 ng/mL). Atazanavir was monitored via electro-spray ionization positive ion mode (ESI+) using the following conditions: i) an ion-spray voltage of 5500 V; ii) temperature, 450 ^{o}C; iii) curtain gas (CUR; set at 10) and Collisionally Activated Dissociation (CAD; set at 5) gas were nitrogen; iv) Ion Source gas one (GS1) and two (GS2) were set at 20; v) entrance potential was set at 10.0 V; vi) quadruple one (Q1) and (Q3) were set on Unit resolution; vii) dwell time was set at 200 msec; and viii) declustering potential (DP), collision energy (CE), and collision cell exit potential (CXP) are voltages (V). Compound settings were: atazanavir (parent drug): 705.4 → 168.1 *m/z* and tamoxifen (internal standard, IS): 372.1 → 72.1 *m/z*. Atazanavir metabolite settings are provided in **Table 1**. Ten µL aliquots were injected onto the LC-MS/MS system for all standards and unknowns. The apparent metabolite concentrations (ng/mL) were derived from the

atazanavir standard curve fitted to a $1/x^2$ weighted linear regression with a high correlation coefficient (R^2 = 0.998). Metabolite values were estimates as metabolite reference standards were not available for calibrators and quality control samples.

***In vivo* plasma samples:** Plasma samples from the *in vivo* study (Anderson et al, 2009) were analyzed for atazanavir metabolites. The measurement of metabolites in the present study was reviewed by the Colorado Multiple Institutional Review Board under the original protocol and was approved. All participants provided written informed consent. Samples from fourteen of the original thirty-one individuals were selected for these analyses; subjects were chosen to most efficiently and economically evaluate whether atazanavir metabolites were comparable in the NAA and AA subjects who expressed CYP3A5 versus those who did not. The subjects included five NAA's not expressing CYP3A5 (Group 1); four NAA expressors (Group 2); and five AA expressors (Group 3). Time points for the atazanavir metabolite analysis included the 2, 4, 12, and 24 hour post-observed-dose samples in order to evaluate points along the entire AUC profile; the 24-hour value was also used for the 0 hour value given the steady-state conditions. Atazanavir concentrations in these samples were not re-quantified with the LC-MS/MS method; many samples were higher than the linear range, so the reported concentrations are those generated previously using a validated HPLC-UV method (Anderson et al, 2009).

To ensure a homogeneous mixture, plasma samples were allowed to warm to room temperature (10 min) followed by vortex mixing (5 s). Samples were removed (100 µL) and transferred into individual micro-centrifuge tubes (500 µL). An extraction solution (200 µL; 2:2:1; methanol:acetonitrile:water) containing 40 ng/mL tamoxifen (IS) was added. The tubes were capped, vortex mixed (5 s), set aside for 5.0 min, and subsequently centrifuged at 13,000

rpm (5.0 min). The supernatants were transferred into individual wells of a 96-well plate, capped, and placed into the auto-sampler cool stack (6.0 ± 0.1 ^{o}C) for analysis.

Data Analyses: Metabolite AUC values were estimated with the linear trapezoidal method. All the atazanavir PK data were reported as part of the parent study and are re-summarized briefly in this report. The metabolite AUC was normalized by atazanavir AUC to produce metabolite:atazanavir AUC ratios for comparisons. Prism 4.02^{TM} (GraphPad Software, Inc.; San Diego, CA) was used for graphing and statistical analysis. One-way ANOVA, followed by a Tukey's multiple comparison tests, were used for comparisons.

Results

***In vitro* liver microsome experiments:** In the presence of NADPH, atazanavir was observed to undergo five different 'Phase I Biotransformation' pathways via human liver microsomal incubations (**Figure 1**). These five pathways produced 16 metabolites (**Table 1**) including i) mono-oxidation (**M1**-**M4**), ii) oxidative decarboxylation (**M5**-**M6**), iii) oxidative dehydration (**M7**-**M8**), iv) mono-oxidation plus oxidative de-carboxylation (**M9**-**M12**); and v) di-oxidation (**M13**-**M16**) (supplementary material, **Figure S1**). Six predominant metabolites (major) were identified (**Figure 2**) with mono-oxidation metabolites **M2** and **M1** being most prevalent. The human CYP3A4 and CYP3A5 incubations produced nine and eight metabolites, respectively and represent all five biotransformation pathways (**Table 1** and supplementary material, **Figures S2**-**S3**).

Given the significant inhibitory effect of ritonavir on atazanavir clearance *in vivo*, the effect of ritonavir on atazanavir intrinsic clearance (CL_{int}) was probed *in vitro*. Atazanavir (1.0 µM at 0.2 mg liver microsomal protein; pool of 50, mixed gender) was incubated in the presence of varying concentrations of ritonavir. Ritonavir (0.5 µM) modified the *in vitro* CL_{int} from 139.8 ± 4.2 (control) to 70.4 ± 10.0 µL/min/mg protein (0.5 µM ritonavir; $P<0.001$, supplementary material, **Figure S4**). Human CYP3A4 and CYP3A5 incubations were probed for metabolite formation differences. As summarized in **Figure 3**, there were notable differences observed between CYP3A4 and CYP3A5. On a pmol CYP comparison, CYP3A5 produced the mono-oxidation metabolites **M1** and **M2** at a faster rate than CYP3A4; 32-fold and 2.6-fold faster for **M1** and **M2** at the 30 min time point, respectively. Other differences include: i) that CYP3A4 produced about equal amounts of **M5** and **M6**, while CYP3A5 favored the formation of **M5**; and ii) CYP3A4 produced **M3** and **M4**, whereas CYP3A5 favored the formation of **M3** over **M4**.

Both CYP3A4 and CYP3A5 incubations showed the formation of **M7**, **M9**, and **M15**. The minor metabolites formed were not appreciably different between the two isoforms (supplementary material, **Figure S5**). A comparison of HLM's from i) a pool of 50 mixed gender, ii) an individual (male) with genetically-determined CYP3A5 non-expression (*3/*3), and, iii) an individual (female) with genetically-determined CYP3A5 expression (*1/*1) demonstrated faster formation of **M1** and **M2** according to the presence of CYP3A5 (**Figure S6**). Given that CYP3A5 produced the major mono-oxidation metabolites **M1** and **M2** at a faster rate than CYP3A4 (**Figure 3**), these metabolites were the focus in the analysis of the *in vivo* plasma samples.

***In vivo* metabolites:** Metabolites **M1** – **M9** (**Table 1**) were identified in *in vivo* samples (supplementary material, **Figure S7**). In terms of the major mono-oxidation metabolites **M1** and **M2**, the *in vivo* plasma samples displayed lower assay signals for **M1** relative to **M2**, consistent with the *in vitro* observations. Atazanavir PK parameters from the parent study and metabolite AUCs and AUC ratios are summarized in **Table 2** (Anderson, et al. 2009). On average, the atazanavir AUC was 1.8-fold higher in NAA-NE individuals (Group 1) compared to NAA-E individuals (Group 2; $P<0.05$). However, the AUCs in AA-E (Group 3) were 2.4-fold higher than NAA-E (Group 2; $P<0.01$), and not significantly different from NAA-NE (Group 1; **Table 2**).

Despite these significant ATV differences in African Americans versus non-African Americans CYP3A5 expressors (Groups 2 and 3), the **M1/ATV** (**Figure 4**) and **M2/ATV** (**Figure 5**) AUC ratios were similar ($P>0.05$) in these two groups. The **M1** ratio values for both CYP3A5 expressor groups were about 2-fold higher than the CYP3A5 non-expressing individuals (**Figure 4**; 0.24 and 0.23 versus 0.10; $P<0.001$, both comparisons). The **M2** ratio

DMD Fast Forward. Published on December 9, 2010 as DOI: 10.1124/dmd.110.036178
This article has not been copyedited and formatted. The final version may differ from this version.

showed a similar relationship where the CYP3A5-expressor groups were about the same (mean 14.0, group 2; and 17.3, group 3; **Figure 5**) and both were about 2-fold higher than the CYP3A5 non-expressing individuals (mean 8.8 group 1; $P<0.05$ and $P<0.001$, respectively). One non-African American who expressed CYP3A5 had an **M2** ratio similar to the non-expressing group, whereas all the **M1** ratios in expressors were above the non-expressors. This observation was consistent with the *in vitro* data where **M1** formation rate was faster via CYP3A5 compared to **M2** (32- versus 2.6-fold, respectively). Taken together, these *in vitro* and *in vivo* data demonstrate a consistent atazanavir metabolite phenotype, particularly the **M1** ratio, which was associated with CYP3A5 expressor status independent of African-American race.

Discussion

The current study was a follow up to an *in vivo* study where atazanavir oral clearance was shown to be dependent on CYP3A5 expression status, but only in non-African Americans (Anderson et al, 2009). As a follow up to this finding, the *in vitro* hepatic metabolism of ATV was investigated first. As summarized in **Table 1** and **Figure 1**, sixteen 'Phase I' metabolites were observed via human liver microsomal incubations. All observed metabolites maintained the 2-(p-tolyl)pyridine functionality; hence all had the daughter ion at 168 *m/z* (**Table 1** and supplementary material, **Figure S8**). Similar daughter fragmentation patterns for atazanavir metabolites have been previously reported (ter Heine et al, 2009). The study by ter Heine et al, which evaluated metabolites in plasma from people taking atazanavir and atazanavir-ritonavir, also showed evidence of major metabolites elucidated in this study (**M1**, **M2**, **M5**, **M6**), but reported a *N*-dealklation and keto-metabolite not readily observed in the present study. A keto-metabolite was also reported among three metabolites in the manufacturer's briefing document (BMS, 2003). The metabolite structures were not reported in the briefing document. No metabolites were described that retained antiretroviral activity. The present study evaluated only the metabolites elucidated in the in vitro studies, so the *N*-dealklation and keto-metabolite – which were not detected in vitro – were not monitored in the in vivo samples. The sixteen metabolites from HLM in the present study were generated from five main pathways: four were mono-oxidation products (M + O; M + 16 atomic mass units (amu); **M1** – **M4**), two were oxidative de-carboxylation products (M – 56 amu; **M5** – **M6**), two were oxidative dehydration products (M – 2 amu; **M7** – **M8**), four were oxidation with oxidative decarboxylation (M – 42 amu; **M9** – **M12**), and four were di-oxidation products (M + 32 amu; **M13** – **M16**). The observed formation of **M5** – **M6** and **M9** – **M12** warrants additional discussion. These

metabolites require the destruction of a carbamate functional group (*i.e.* one of two present in atazanavir). While this chemical transformation might represent general hydrolysis or catalyzed via esterase activity, atazanavir incubates (37 ^{o}C, 2 hr) in the presence of HLM's without NADPH did not reveal carbamate hydrolysis (data not shown). This suggests that these metabolites were produced via a CYP catalyzed oxidative de-carboxylation mechanism (**Figure 1**); a CYP catalyzed pathway analogous to that proposed for loratadine to generate descarboethoxyloratadine (DCL) (Yumibe et al, 1996). Six major atazanavir metabolites were identified (**Figure 2**). Mono-oxidation products, **M1** and **M2** were most prevalent via HLM. In addition, HLM's were used to probe the effect(s) of ritonavir on atazanavir metabolism. Ritonavir (0.50 µM) was shown to decrease atazanavir (1.0 µM) *in vitro* CL_{int} by 2-fold (Supplementary material, **Figure S4**), consistent with ritonavir's effect on atazanavir CL/F *in vivo* (Anderson et al, 2009). A limitation to the metabolite analyses was the lack of metabolite reference standards. Therefore, the atazanavir standard curve was used to estimate metabolite concentrations; an approach to determine relative metabolite signals, but not a true quantification of metabolite concentrations.

Human CYP3A4 and human CYP3A5 incubates produced evidence for all five phase I biotransformation pathways (**M1**, **M2**, **M5**, **M6**, **M7**, **M9** and **M15**). Similar to HLM's, metabolites **M1** and **M2** were major and formed in a linear time-dependent fashion in human CYP3A4 and CYP3A5 incubates (**Figure 3**). Notable differences between CYP3A4 and CYP3A5 were observed. Most significantly, CYP3A5 produced the major mono-oxidation metabolites **M1** and **M2** at a significantly faster rate than CYP3A4; ~32-fold faster for **M1** and 2.6-fold faster for **M2**. A faster rate was also observed in HLM from a genetically-determined CYP3A5 expressor (*1/*1) versus that from a genetically-determined CYP3A5 non-expressor

(*3/*3) (**Figure S6**). It should be noted that atazanavir itself is a CYP3A inhibitor as measured by inhibition of triazolam hydroxylation in HLM (Perloff 2005). The relative inhibition of atazanavir on CYP3A4 versus CYP3A5 was not evaluated in this study and it is not clear whether auto-inhibition may influence the metabolite formation profiles. Nevertheless, the present study demonstrated metabolite formation differences between CYP3A4 versus CYP3A5 in vitro and observed consistent metabolite findings in humans receiving atazanavir.

The goal of the present study was to characterize the metabolite phenotype in individuals who express CYP3A5, and to also compare this phenotype between the AA's and NAA's who express CYP3A5. As demonstrated in **Figure 4** and **5**, the **M1** and **M2** metabolite ratios were higher in those who expressed CYP3A5, regardless of race. Of these two metabolites, the **M1** ratio in the *in vivo* samples showed the most consistent metabolite phenotype (**Figure 4**), results which were consistent with the *in vitro* data. The consistent metabolite findings suggest that other biological differences are driving the different atazanavir exposures in African Americans versus non-African Americans who express CYP3A5 (**Table 2**). ABCB1 (encoding the P-gp efflux transporter) genotypes were evaluated in the parent study and found to be associated with atazanavir PK. However, the small sample sizes in the AA's versus NAA groups expressing CYP3A5 (n=5 and n=4, respectively) limits the ability to attribute atazanavir PK differences to P-gp genetics on the background of CYP3A5 expression. Other possibilities include differences in intake or other efflux transporter function/expression (Rodriguez-Novoa et al, 2007; Lubomirov et al, 2010), differences in transcription factors for metabolic activity (Siccardi et al, 2008), or differences in acidity of the stomach influencing drug absorption (unlikely as standardized meals were given in the parent study and subjects taking antacids were excluded) (Zhu et al, 2010). It should be noted that atazanavir metabolite AUC ratio is dependent on metabolite formation and

metabolite clearance. The in vitro studies demonstrated **M1** and **M2** formation rate differences for CYP3A5 relative to CYP3A4. Although the study was not designed to quantify metabolite distribution volume and clearance, there was no difference in the in vivo metabolite half-life between CYP3A5 expressors versus non-expressors (data not shown), which suggests that metabolite clearance was not influenced by CYP3A5 expression.

In conclusion, this study provides evidence for a consistent metabolite phenotype for atazanavir in genetically determined CYP3A5 expressors, regardless of race. This was relevant for understanding atazanavir pharmacology in terms of CYP3A5 expression status observed in a previous study. This study also illustrates the apparent, and important, contribution of other factors on atazanavir PK even within individuals expressing CYP3A5. African American race appears to be a predictor for the presence of these other pharmacologic factors. Future pharmaco-genomic studies with atazanavir should sample from diverse populations and assess CYP3A5 expressor status along with other pharmacologic variables in order to gain the most complete picture of atazanavir disposition in humans.

Acknowledgements: The authors wish to thank the investigators, personnel, and study volunteers who assisted with the parent study and Dr. Jennifer Kiser for helpful comments on the manuscript.

Authorship Contributions: Drs. Wempe and Anderson conceived the study idea, planned the analyses, analyzed the data, and wrote the manuscript. Dr. Wempe designed and performed the in vitro experiments.

References

Anderson PL, Aquilante CL, Gardner EM, Predhomme J, McDaneld P, Bushman LR, Zheng JH, Ray M, MaWhinney S (2009) Atazanavir pharmacokinetics in genetically determined CYP3A5 expressors versus non-expressors. *J Antimicrob Chemother* **64**: 1071-9.

Bristol-Myers Squibb Company (BMS). BMS-232632 Atazanavir Briefing Document May-2003. (2003) Available at: http://www.fda.gov/ohrms/dockets/ac/03/briefing/3950B1_01_BristolMyersSquibb-Atazanavir.pdf. Accessed November 4, 2010.

Croom KF, Dhillon S, Keam SJ. (2009) Atazanavir: A Review of its Use in the Management of HIV-1 Infection. *Drugs* **69**: 1107-40 10.2165/00003495-200969080-00009.

Lubomirov R, di Iulio J, Fayet A, Colombo S, Martinez R, Marzolini C, Furrer H, Vernazza P, Calmy A, Cavassini M, Ledergerber B, Rentsch K, Descombes P, Buclin T, Decosterd LA, Csajka C, Telenti A; Swiss HIV Cohort Study (2010) ADME pharmacogenetics: investigation of the pharmacokinetics of the antiretroviral agent lopinavir coformulated with ritonavir. *Pharmacogenetics and Genomics*; **20**: 217-30 10.1097/FPC.0b013e328336eee4.

Obach RS (1999) Prediction of human clearance of twenty-nine drugs from hepatic microsomal intrinsic clearance data: An examination of in vitro half-life approach and nonspecific binding to microsomes. *Drug Metab Dispos* **27**: 1350-9.

Perloff S, Duan S, Skolnik P, Greenblatt D, von Moltke L. Atazanavir: Effects on P-glycoprotein and CYP3A Metabolism in vitro. *Drug Metab Dispos* **33**: 764-770.

Rodríguez-Nóvoa S, Martín-Carbonero L, Barreiro P, González-Pardo G, Jiménez-Nácher I, González-Lahoz J, Soriano V (2007) Genetic factors influencing atazanavir plasma concentrations and the risk of severe hyperbilirubinemia. *Aids* **21**: 41-6.

Siccardi M, D'Avolio A, Baietto L, Gibbons S, Sciandra M, Colucci D, Bonora S, Khoo S, Back DJ, Di Perri G, Owen A (2008) Association of a single-nucleotide polymorphism in the pregnane X receptor (PXR 63396C-->T) with reduced concentrations of unboosted atazanavir. *Clin Infect Dis* **47**: 1222-5.

ter Heine R, Hillebrand MJ, Rosing H, van Gorp EC, Mulder JW, Beijnen JH, Huitema AD (2009) Identification and profiling of circulating metabolites of atazanavir, a HIV protease inhibitor. *Drug Metab Dispos* **37**: 1826-40.

Yumibe N, Huie K, Chen KJ, Snow M, Clement RP, Cayen MN (1996) Identification of human liver cytochrome P450 enzymes that metabolize the nonsedating antihistamine loratadine. Formation of descarboethoxyloratadine by CYP3A4 and CYP2D6. *Biochem Pharmacol* 1996; 51: 165-72.

Zhu L, Persson A, Mahnke L, Eley T, Li T, Xu X, Agarwala S, Dragone J, Bertz R. (2010) Effect of Low-Dose Omeprazole (20 mg Daily) on the Pharmacokinetics of Multiple-Dose Atazanavir With Ritonavir in Healthy Subjects. *J Clin Pharmacol*.

Footnotes

Funding for this research was through the Medicinal Chemistry Core facility via the Colorado Clinical and Translational Sciences Institute grant from National Center for Research Resources at the National Institutes of Health [5UL1RR025780], and via internal funds from the Department of Pharmaceutical Sciences.

[1] The terms “Expressor” and “Expresser” have both been used in scientific literature to describe persons who express CYP3A5 protein.

DMD Fast Forward. Published on December 9, 2010 as DOI: 10.1124/dmd.110.036178
This article has not been copyedited and formatted. The final version may differ from this version.

Legends for Figures.

Figure 1. Proposed atazanavir metabolite pathways (major and minor) commonly observed via human liver microsomal, CYP3A4 or CYP3A5 incubates, and via human *in vivo* samples.

Figure 2. Major atazanavir metabolites observed in human liver microsomes *in vitro* incubations (0 – 30 min); ■ = **M1**, ▲ = **M2**, ▼= **M5** & **M6**, ○ = **M7**, ● = **M9**. Data n = 6 ± SD.

Figure 3. Major atazanavir metabolites observed via human CYP3A4 and CYP3A5 *in vitro* incubations (0 – 30 min); □ = **M1** (CYP3A4), ■ = **M1** (CYP3A5), ∆ = **M2** (CYP3A4), ▲ = **M2** (CYP3A5); data n = 4 ± SEM.

Figure 4: Metabolite **M1** to atazanavir AUC ratios in the three groups: group 1 (G1), non-African American CYP3A5 non-expressors; group 2 (G2), non-African American CYP3A5 expressors; group 3 (G3), African American CYP3A5 expressors; data ± SEM.

Figure 5: Metabolite **M2** to atazanavir AUC ratios in the three groups: group 1 (G1), non-African American CYP3A5 non-expressors; group 2 (G2), non-African American CYP3A5 expressors; group 3 (G3), African American CYP3A5 expressors; data ± SEM.

DMD Fast Forward. Published on December 9, 2010 as DOI: 10.1124/dmd.110.036178
This article has not been copyedited and formatted. The final version may differ from this version.

Table 1 Atazanavir metabolite summary

Analyte	Time (min)	Phase I Transformation	ESI (+) *m/z*	HLM	3A4	3A5	*in vivo*
Atazanavir	18.0	None	705.4 --> 168.1	Y	Y	Y	Y
M1	16.9	MO	721.4 --> 168.1	Y	Y	Y	Y
M2	17.1	MO	721.4 --> 168.1	Y	Y	Y	Y
M3	17.6	MO	721.4 --> 168.1	Y	Y	Y	Y
M4	18.1	MO	721.4 --> 168.1	Y	Y	ND	Y
M5	14.6	O-Decarb	647.4 --> 168.1	Y	Y	Y	Y
M6	14.7	O-Decarb	647.4 --> 168.1	Y	Y	Y (t)	Y
M7	18.0	O-Deh	703.4 --> 168.1	Y	Y	Y	Y
M8	17.2	O-Deh	703.4 --> 168.1	Y	ND	ND	Y
M9	17.9	MO + O-Decarb	663.4 --> 168.1	Y (t)	Y	Y	Y
M10	12.4	MO + O-Decarb	663.4 --> 168.1	Y	ND	ND	ND
M11	12.8	MO + O-Decarb	663.4 --> 168.1	Y	ND	ND	ND
M12	13.9	MO + O-Decarb	663.4 --> 168.1	Y	ND	ND	ND
M13	15.0	DO	737.4 --> 168.1	Y	ND	ND	ND
M14	16.0	DO	737.4 --> 168.1	Y (t)	ND	ND	ND
M15	16.4	DO	737.4 --> 168.1	Y	Y (t)	Y (t)	ND
M16	16.9	DO	737.4 --> 168.1	Y	ND	ND	ND

Y = Detected; t = trace amount observed; ND = not detected; HLM = human liver microsomes

MO = mono-oxidation; DO = di-oxidation,

O-Decarb = Oxidative Decarboxylation; O-Deh = Oxidative Dehydration

DMD Fast Forward. Published on December 9, 2010 as DOI: 10.1124/dmd.110.036178
This article has not been copyedited and formatted. The final version may differ from this version.

Table 2: Metabolite and atazanavir (ATV) concentrations for *in vivo* samples.

Subject Group	ATV AUC µg•h/mL	M1 AUC ng•h/mL	M2 AUC ng•h/mL	M1:ATV Ratio*	M2:ATV Ratio*	ATV CL/F (L/hr/kg)
1	33.2	2.9	270	0.09	8.1	0.13
1	24.9	2.0	207	0.08	8.3	0.18
1	17.7	2.4	151	0.14	8.6	0.25
1	32.8	3.3	300	0.10	9.2	0.16
1	17.4	2.0	169	0.11	9.8	0.22
Ave	**25.2**	**2.5**	**219**	**0.10**	**8.8**	**0.19**
SD	**7.7**	**0.6**	**64**	**0.02**	**0.7**	**0.05**
2	9.9	1.7	82	0.18	8.3	0.43
2	18.3	3.9	268	0.21	14.6	0.34
2	16.5	4.9	267	0.29	16.2	0.37
2	10.9	3.1	184	0.28	16.9	0.38
Ave	**13.9**	**3.4**	**200**	**0.24**	**14.0**	**0.38**
SD	**4.1**	**1.4**	**88**	**0.05**	**3.9**	**0.04**
3	29.3	6.0	431	0.21	14.7	0.19
3	28.1	6.6	481	0.23	17.1	0.16
3	35.9	8.4	639	0.23	17.8	0.21
3	38.6	8.1	700	0.21	18.1	0.13
3	36.5	9.1	683	0.25	18.7	0.15
Ave	**33.7**	**7.6**	**587**	**0.23**	**17.3**	**0.17**
SD	**4.7**	**1.3**	**123**	**0.02**	**1.6**	**0.03**

Group: 1, non-African American CYP3A5 non-expressors; Group 2, the non-African American CYP3A5 expressors; Group 3, African American CYP3A5 expressors. *Note, for readability, the actual value was 1000 fold lower; the ATV AUC units are µg•h/mL and metabolite units are ng•h/mL.

Figure 1

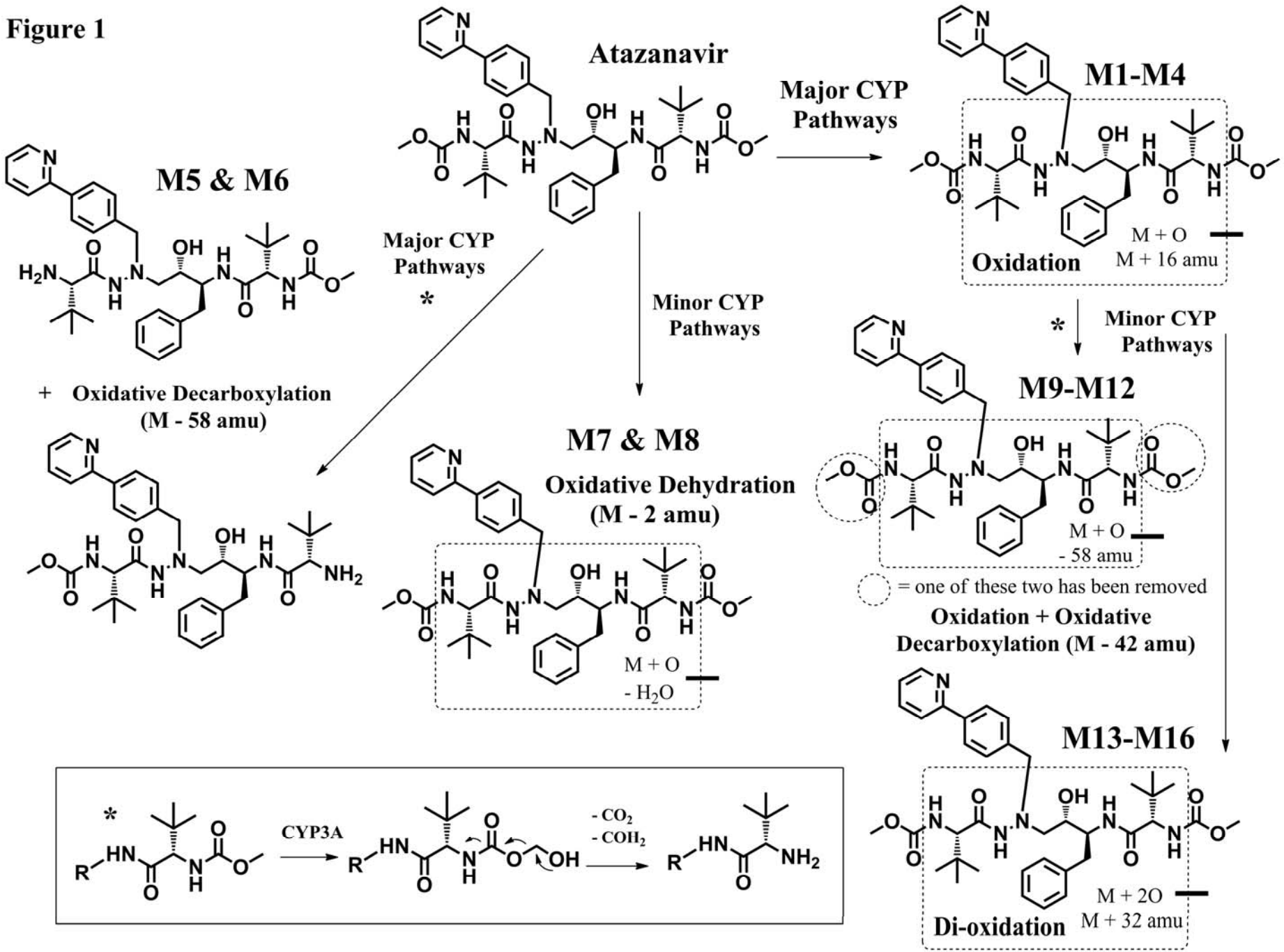

Figure 2

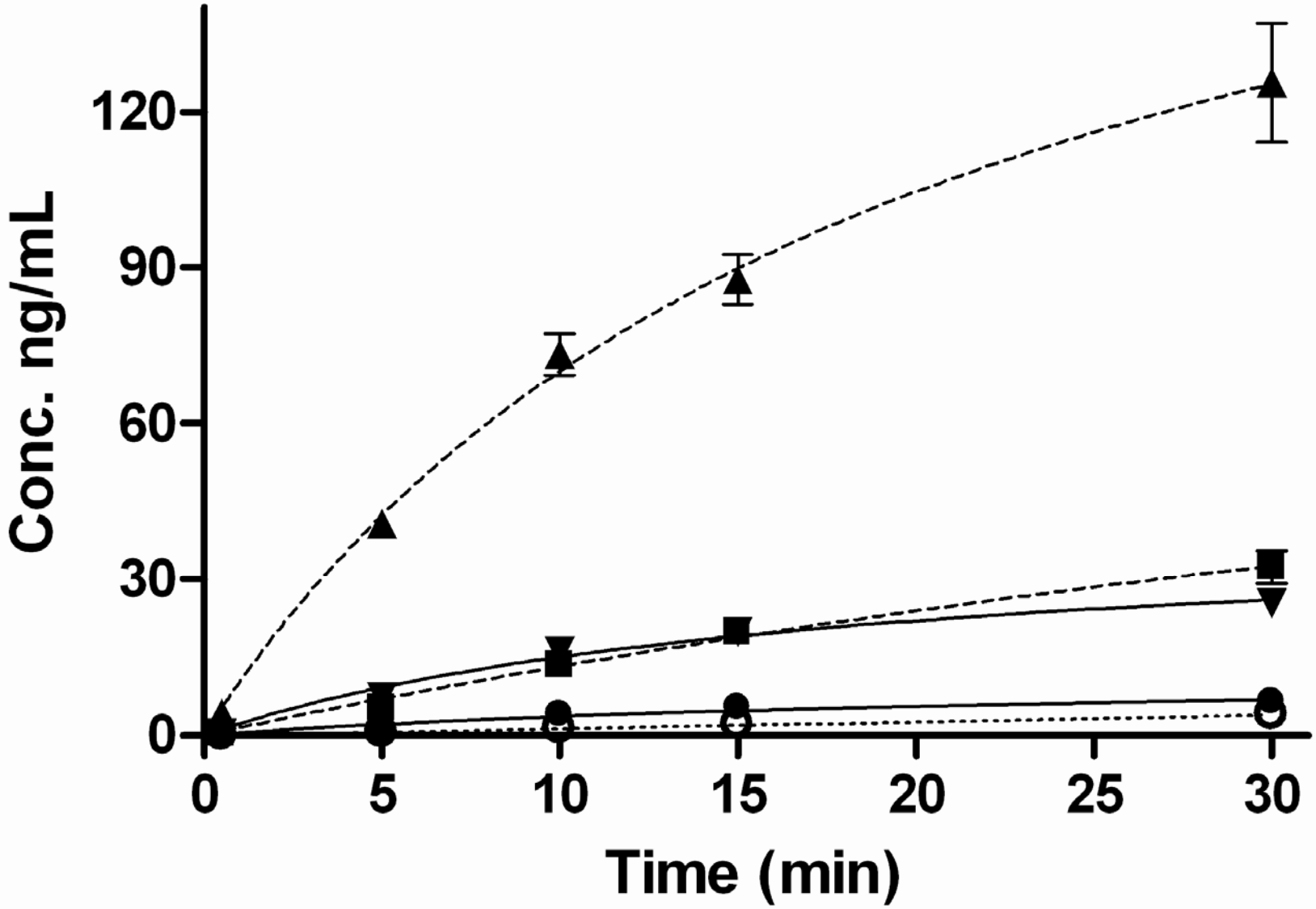

Figure 3

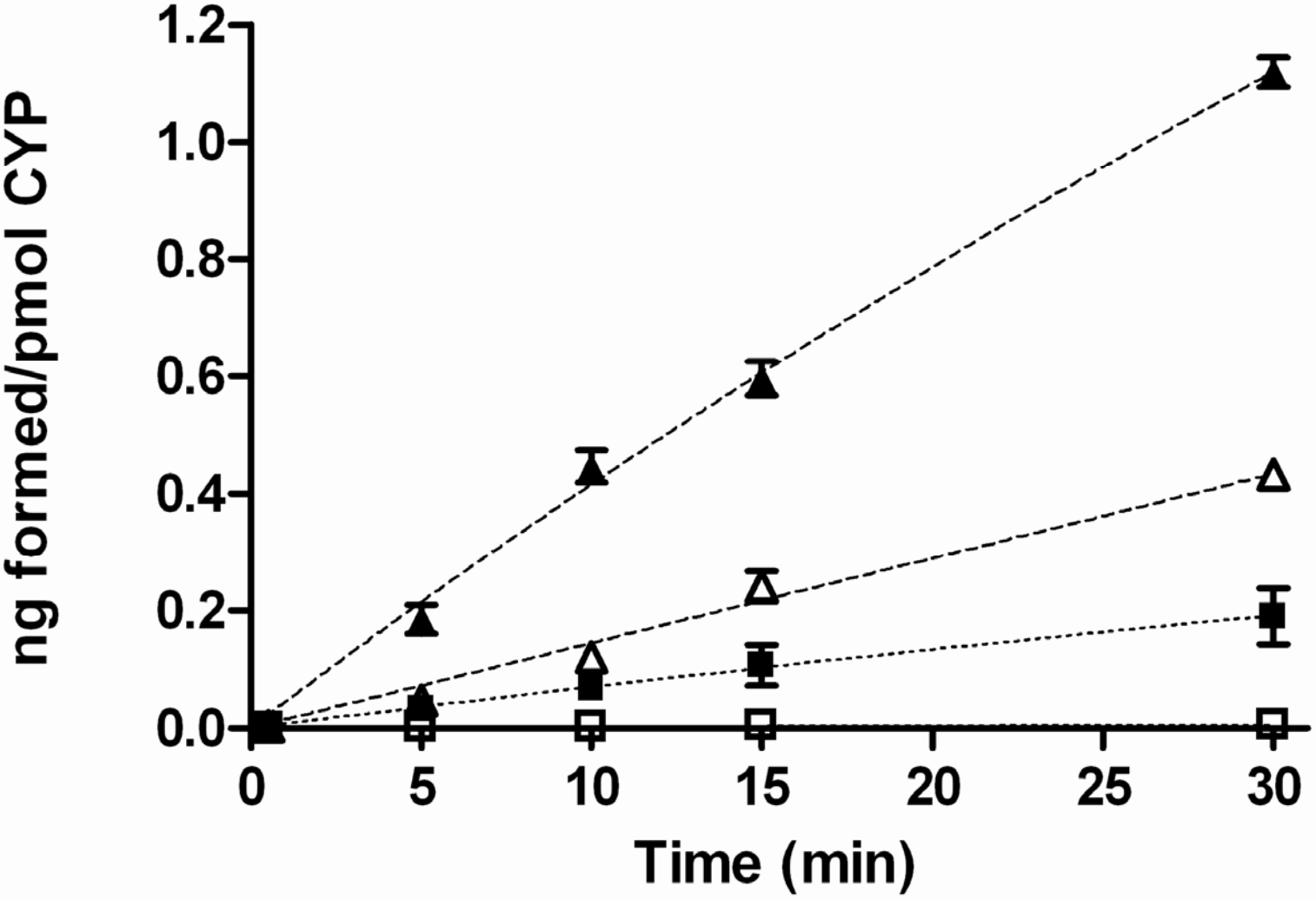

Figure 4

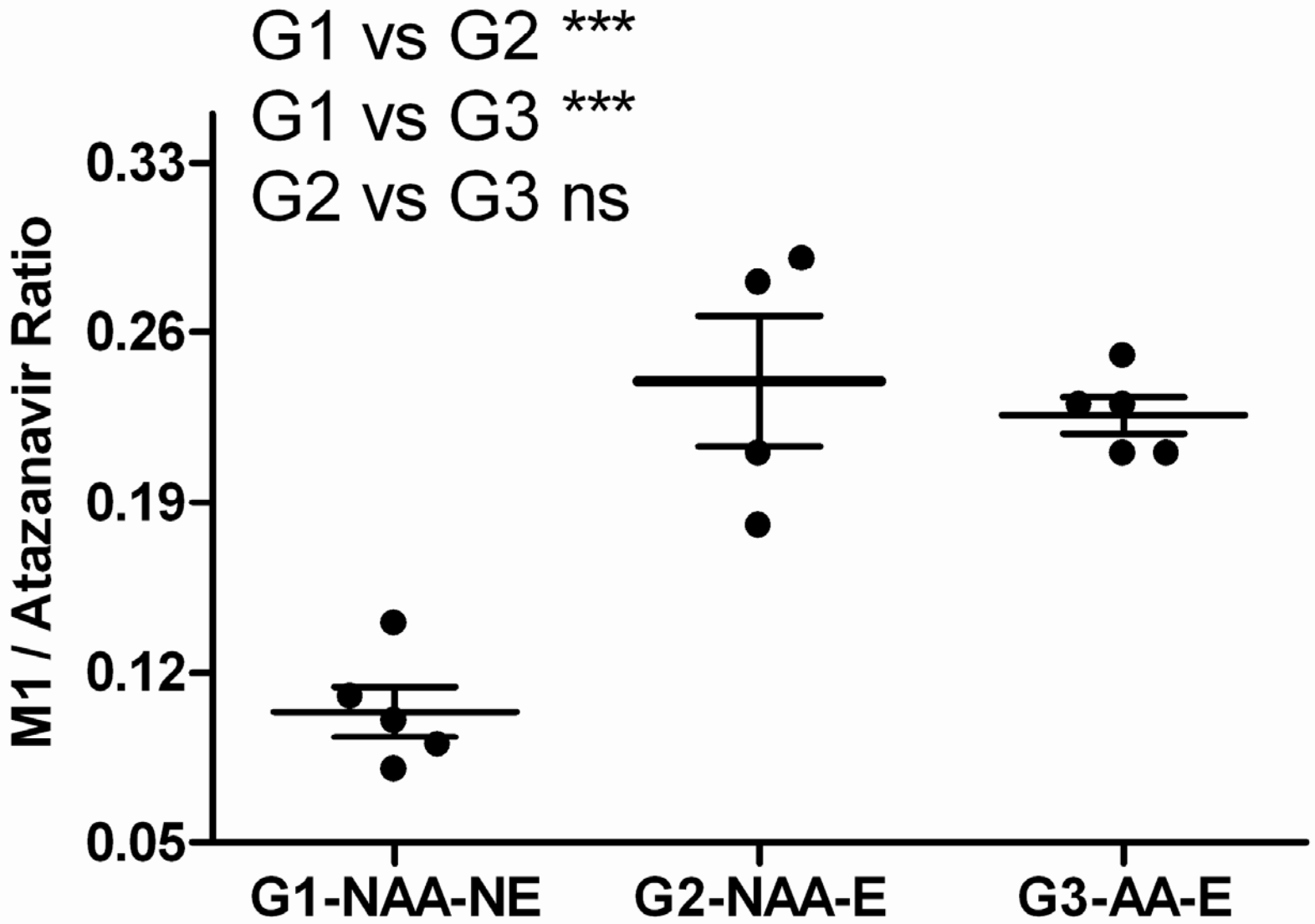

Figure 5